Structure prediction of manganese dioxide nanoclusters using computer simulation techniques

[1]R R Maphanga, [1]P E Ngoepe, [2]C R A Catlow and [2]S M Woodley

Materials Modelling Centre, School of Physical and Mineral Sciences, University of Limpopo, Private bag x 1106, Sovenga, 0727, South Africa

Department of Chemistry, Materials Chemistry, University College London, Kathleen Lonsdale Building, Gover Street, London, WC1E 6BT, United Kingdom

E-mail: rapela.maphanga@ul.ac.za

Abstract. The characteristics of nanoclusters are linked to the high value of their surface/volume ratio, and therefore the structure of nanoclusters plays an important role in determining their physical properties. In order to enhance the properties of MnO_2 for various applications, some new or modified MnO_2 compounds are developed recently. One of the major demands for developing these materials is to modify and strengthen the structural stability in order to prevent the rapid capacity fading during the process of charge/discharge cycling. The interest in synthesis and characterisation of nanoclusters is driven by a wide range of applications of nanoparticle materials in catalysis, electronics and energy conversion. The lowest energy configurations for $(MnO_2)_n$ clusters, n =1 to 4 are predicted, employing the interatomic potential technique and electronic structure density functional theory method at the PBEso10 level. The application of an evolutionary algorithm to different energy landscapes, as defined by interatomic potentials, for each cluster size was used to generate the plausible structures for refinement using DFT. The geometrical properties of different sizes of nanoclusters are investigated. The DFT based, MnO_2 global minima configurations clusters were found to be similar to those predicted for isostructural TiO_2.

1. Introduction

MnO_2 as a well-known transition-metal oxide is one of the most attractive inorganic materials because of its structural flexibility and wide range applications in many chemical processes such as ion exchange, separation, catalysis, molecular adsorption, biosensors and energy storage in batteries and supercapacitors. MnO_2 exists in several crystallographic forms, such as α-, β-, γ-, λ-, δ-, ε–type, where the basic unit (MnO_6) octahedron links in different ways. Most of these systems have been tested for the application in various batteries, such as alkaline battery, lithium metal battery and lithium-ion battery. One of the major demands for developing new materials is to modify and strengthen the structural stability in order to prevent the rapid capacity fading during the process of charge/discharge cycling [1, 2].

Materials at the nanometer scale display different chemical and physical properties from bulk systems. Recently, special attention has been focused on the fabrication of the hierarchically superstructures based on low-dimensional nanocrystals [3], which are expected to play a crucial role in fabricating the next generation of nanodevices because they can be used as both building units and interconnections and will offer opportunities to explore their novel collective optical, mechanical,

magnetic and electronic properties. There has been an increased interest in manganese dioxide nanostructures for their potential applications in catalysis, rechargeable batteries, ion-sieves and supercapacitors. Nanowires, nanorods, nanobelts, nanotubes and nanosheets of MnO_2 have been widely reported. Several experimental methods (such as liquid-phase, thermal decomposition, electrochemical deposition, sol-gel, molten salt) have been developed for the synthesis of MnO_2 nanostructures, including, nanorods, nanowires, nanobelts and nanoneedles, nanosheets. However, experimental organisation of MnO_2 nanosheet clusters into hierarchical super structures still remains a challenge. Feng *et al* [4] explored the preparation of the hierarchical MnO_2 sheets via electrochemical deposition. Recently, low temperature hydrothermal method was used to synthesise uniform nanoclusters of γ–MnO_2. Li ions were treated with MnO_2 nanoclusters without any intercalation to investigate the effect of lithium ions on the morphology, particle size and charge/discharge behaviours of the synthesised MnO_2 nanocusters [5]. It has been found that the solid state treatment can change the morphology and particle size of γ–MnO_2 nanoclusters, without considerable change in the phase composition. In addition, low-dimensional structures of MnO_2 have been synthesised as nanorods, nanosheet [6] and modelled as nanoparticle [7]. In addition, MnO_2 structures have been simulated and studied in varying shapes and architectures, that is, nanosheet, nanorod and mesoporous [8]. The control of morphologies, sizes, architectures, and patterns of nanocrystals have become a dominant theme in material field since these parameters are the key elements that determine physical properties. It is well known that battery performance is highly dependent on MnO_2 morphologies and crystallographic forms.

Low-lying local minima on the energy of formation landscape defined by interatomic potentials (IPs) were found by employing one of a number of global optimisation algorithms [9, 10]. The use of IPs approaches reduces the computational cost of locating plausible structures, which can be refined at a later stage. Searching landscapes based on IPs has been successfully applied to finding a wide range of bulk metal oxide phases [11-15] and therefore such techniques have been applied to clusters, such as, MgO [16], ZnO [17], ZnS [18, 19], TiO_2 [19], SiO_2 [20], ZrO_2 [21], Al_2O_3 [13] and In_2O_3 [22]. The IPs are typically fitted so as to reproduce the structures and properties of the bulk phases, which may be one of the causes of a change in the ranking in terms of stability order for the clusters. When the plausible structures are found, are refined using a DFT approach. The unprecuresedented efforts have focused on the synthesis [23, 24] structure [25, 26] properties [27] and applications [28-30] of nanomaterials. However, structural features that exist at the nanoscale are difficult to characterise experimentally, and therefore, computer simulation methods offer a unique window of exploration into nanomaterials. In this study we develop simulation strategies for generating MnO_2 nanoclusters. To understand the behaviour of MnO_2 small clusters at nanoscale, a combination of global search techniques and density functional theory method are employed to elucidate the energy landscapes and geometrical configurations of MnO_2 clusters.

2. Methodology

Energies of nanoclusters can be calculated using methods based either on interatomic potentials or electronic structure techniques. The interatomic potential (IP) method is computationally inexpensive and allows large numbers and sizes of clusters to be explored. However, they have a number of limitations which may results in giving inaccurate results. Combining the two approaches (interatomic potential and density functional theory) proved to be insightful, where IP methods are being used in the first stage to explore the range of cluster sizes and structures, while DFT methods are used in the second stage to refine the energy ordering and structures of a selected subset of clusters. Thus, those found to be low in energy from the first stage. In addition, the DFT methods can be employed to test the reliability of the first stage calculations by probing cluster structures, which are likely to be sensitive to the parameterisation of interatomic potential used. Interatomic potentials are commonly parameterised by reference to bulk crystalline properties. This may cause difficulties when they are applied to clusters where the coordination number and bonding may differ. It is vital that the potential based calculations are validated by DFT methods.

All IP calculations are based on Born model of ionic solids, in which the Mn and O ions interact via a long range Coulombic interactions and short-range parameterised interactions. The potential parameters were previously developed by Matsui and were refined and used to model bulk, surfaces and structures of MnO_2 [7, 8, 31]. For the shell model, potentials developed by Ammundsen [32] were employed and fitted to reproduce the lattice parameters of MnO_2 bulk structures. The potentials gave good agreement with the crystal structures of both pyrouliste and ramsdellite polymorphs of MnO_2. The evolutionary algorithm implemented within the GULP [33] code was used to perform IP calculations. The IP calculations are based on two potential models, namely, the partially charged rigid ion model and the fully charged shell model. The energy is given by the sum of the two-body interactions and its analytical expression is given below:

$$V(r_{ij}) = \frac{q_i q_j}{r_{ij}} + B_0 + B_1 r + B_2 r^2 + B_3 r^3 + B_4 r^4 + B_5 r^5 \quad (1)$$

where the first term is the Coulomb contribution to the energy between two point charges q_i and q_j at distance r_{ij} apart. The analytical expression for Buckingham potential employed in this work, describes the interaction between two ions, *i* and *j*, of charge q separated by a distance r and is given in equation below:

$$Ur_{ij} = \left[\frac{q_i q_j}{r_{ij}} + A_{ij} e^{\left(-r_{ij}/\rho_{ij}\right)} - \frac{c_{ij}}{r_{ij}^6}\right] \quad (2)$$

An evolutionary algorithm (EA) method for global optimisation in stage 1 was employed to search for lower Local Minima (LM) on the energy hypersurface to predict stable and low-energy metastable atomic configurations. Different relaxed configurations, initially random stationary points on the energy hypersurface, from a population in which competition to survive and procreate is simulated. The probability of success on any current configuration is based on its energy relative to the other configurations in the population. In the current study, only the best 30 unique structures are kept, at the end of each cycle. Within a population, if the difference in the energy of formation between the two configurations is within E_d, then the higher energy configuration is removed from the population. The EA method was applied at least twice to each hypersurface, when E_d = 0.01 eV and E_d = 0.004 eV. On each of these standard runs, 200 EA cycles were performed. The atoms of each isolated cluster are constrained to be within a spherical container with a radius of 8 Å. The constraint prevents any initial fragmentation of a cluster and helps to speed up convergence of the local optimiser. Each LM corresponds to a configuration of atoms of the cluster, referred to as plausible structure.

As a second stage, each set of plausible structures for the IP are refined using standard local optimisation techniques. In the final stage the global minima structures and a number of metastable local minima configurations as defined by the IPs, were refined using a DFT method. The DFT (PBEsol) all-electron method with a local numerical orbitals basis set and local optimisation techniques as implemented in the FHI-AIMS [34] was employed. The FHI-AIMS two-tiered basis set was employed for the oxygen atoms and only the first-tier basis set for the manganese atoms and scalar-relativistic effects treated at the scaled ZORA level. To improve the energies and the respective electronic structures, the hybrid PBEsol0 functional and the full ZORA level of the theory were employed for recalculation. Configurations in the final population of the evolutionary algorithm are refined using the shell model. Then 30 lowest energy candidate structures, as measured by the energy of formation using the rigid ion and the shell models, were then subjected to geometry optimisation using DFT.

3. Results and Discussions

The lowest energy local minima configurations for $(MnO_2)_n$ n=1-4, clusters have been published previously, where the order of stability as measured by IP and DFT PBEsol0 methods were presented [35]. In addition, the saddle point configurations for MnO_2 in comparison with global minima for TiO_2

clusters were reported. Figure 1 shows the most stable $(MnO_2)_n$ n=1-4 nanoclusters in comparison to literature results.

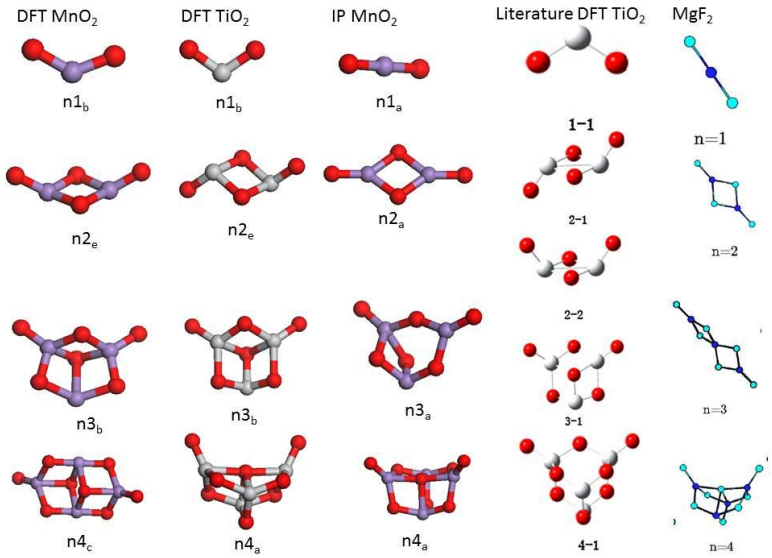

Figure 1: Geometrical configuration of MnO_2 nanoclusters in comparison with nanoclusters from the literature, obtained using IP and DFT methods.

In similar approach used to determine MO_2 (M=Ti, Zr, Hf, Si) clusters, to that discussed above for obtaining low-energy structures, the one key point is that the influence of the d-electrons is not usually accounted for in models based on interatomic potentials (IPs), i.e. when searching for plausible structures. In this study, the d-electrons are accounted for when searching for plausible structures. Thus, the spin configuration is incorporated within IP calculations. Typically, this influence has a greater effect on the bond angles about under-coordinated atoms on the surface, which can always be corrected for in a later stage, e.g. further refinements of the plausible structures using DFT approaches.

For n = 1, interatomic potential predicts a linear configuration with an angle of 180° during stage 1. This is in agreement with previous studies on MgF_2 clusters [36]. The structure bends into a boomerang (n1a) during relaxation in stages 3 and 4 when the DFT methods are employed. During DFT relaxation, the bond angle tends to decrease from 180° to 129° because polarisation is explicitly included in DFT models. Previously, different basis sets (ECP and DZV) have been employed to calculate geometries for isostructural TiO_2 and they gave similar results except small differences in bond lengths and angles [37]. They found that IP predicted a linear configuration with an angle of 180° while B3LYP/6 predicted an angle of 110.41°. Thus, n=1 TiO_2 nanocluster, the geometry was predicted to be of angular configuration. As it has been reported for isostructural TiO_2, our results predict the same configuration. Currently, there are no literature results on MnO_2 nanoclusters to compare with. Previous studies reported that d-orbitals have influence on the nanocluster arrangement. Thus, smallest global minima configurations for germania, silica and stania have a linear arrangement whilst titania, hafnia and zirconia have a boomerang arrangement. Similar local minima configurations for DFT calculations have been found for MnO_2 nanoclusters even though bond angles associated with any singly coordinated atoms are typically different.

The interatomic potential predicts $n2_a$ to be the global minimum, which has planar arrangement with bond distance of 1.687 Å for Mn-O1 and 1.822 Å for Mn-O2. The configuration depicts that oxygen atoms form a square on the mirror plane between the two manganese atoms. The IP predicts the GM structure to be the same as those previously reported for silica, germania, stania [21] and MgF_2 smallest cluster configurations. In stage 3 where the global minima found in stage 1 is relaxed, $n2_e$ $n2_b$ and $n2_c$ configurations are found to be the local minima. When the DFT method is employed to relax plausible structures, $n2_b$ and $n2_a$ configurations are obtained as the global minima for MnO_2 and TiO_2 clusters, respectively. The models predict the bond distances of the two Mn-O1 pair to be

smaller than that of four Mn-O2. For n = 2 global minima clusters, IP geometries predict bond distance results that are closely comparable to DFT results. Both systems predict a configuration with two-terminal Mn-O bond as the global minima in agreement with previous studies on TiO_2 DFT nanoclusters calculations. The first and second local minima are predicted to be the configurations with two terminal Ti-O and one terminal and three bridging O atoms respectively. Comparing the IP configurations for $(MnO_2)_2$ nanoclusters with those obtained using DFT, the atomic arrangement is similar with DFT configurations bending to form a quasi-like isomer for the first two local minima, i.e., $n2_e$ and $n2_b$.

The cluster n3A was predicted to be the global minima for IP calculations. The bond lengths and angles for this cluster are also listed in table 1, where O1 and O2 indicate that oxygen atoms is coordinated to 1 and 2 manganese atoms respectively. The lowest energy configuration, $n3_b$ for $(MnO_2)_3$ is composed of two terminal oxygen atoms and one three-fold coordinated oxygen atoms in agreement with previous DFT calculations. The DFT predicts that the GM configuration is composed of three tetragonal sides of a cuboid with two singly coordinated oxygen atoms. The cluster n3c has the same topology, except that one bond is missing to complete a three-fold coordinated oxygen atoms. The third lowest-energy configuration depicts a quasi-like isomer with two orthogonal MnO_2. The quasi-linear arrangement was suggested to be the global minimum in the Hatree-Fock [38] and pair-potential [39] calculations, whilst n3c was suggested as the global minimum in recent pair potential studies [37]. The local minima configurations are found to be of the same arrangement with the global minima, in which one Mn-O bond is broken. Similarly, DFT calculations for the nanocluster n=3, predicts the configuration of the lowest GM to be identical to those found for TiO_2, ZrO_2 and HfO_2 in previous studies. Thus, $n3_b$ is the same GM as reported for the aforementioned nanoclusters. The GM configuration for DFT-PBEsol0, can be constructed from smaller clusters, in particular, $n1_b$ and $n2_b$. Thus, the smallest lowest energy configurations can be used as building blocks for the larger clusters.

The configuration n4e is found to be the global minima for $(MnO_2)_4$, which is composed of two terminal oxygen atoms and six bridging oxygen atoms. The GM configurations found for n=4 can be constructed from smaller clusters. Numerous DFT studies on $(TiO_2)_n$ showed that DFT calculations predict the lowest energy global minima better than the other methods, such as Hatree-Fock (HF) and pair-potential. The latter two methods neglect the partial covalent nature of Ti-O bonds. The comparison of the lowest three LM MnO_2 cluster structures and those predicted for titania and zirconia is noted that the same configurations and rank is found for n = 2. The clusters are ranked according to PBEsol0 functional because it is one of the least biased, among complementary functionals. The small clusters are isostructural to those predicted for titania, silica and hafnia [21] and characterised by Mn ions concentrating in the core region of the cluster decorated by dangling, or singly coordinated, oxygen ions at the periphery. However, when the energy of formation is calculated using a DFT approach, after relaxation, the dangling oxygen atoms for MnO_2 do not remain in the plane containing the nearest Mn_2O_2 tetragon.

4. Conclusion

Interatomic potential and density functional theory methods were employed successfully to predict the global and local minima configurations of small $(MnO_2)_n$ n=1-4 nanoclusters. The IP method allows a large number of configurations to be explored. The plausible structures are then refined using more accurate DFT-PBEsol0 method. There is a good agreement between our generated MnO_2 nanocluster results and literature results for other metal oxides, in particular, isostructural TiO_2. The IP and DFT methods predict LM configurations for $(MnO_2)_n$ n=1-4 to be similar to those reported for TiO_2 obtained using Hybrid Simulated Annealing-Monte Carlo Basin Hopping (SA-MCBH) and DFT (B3LYP/DZVP) respectively. For these small clusters, the two methods predict similar global minima configurations with slight difference in bond angles. It is noted that all the lowest-energy clusters always possess one or two terminal Mn-O bonds of almost a length of approximately 1.6Å. The results are of great importance in understanding the formation and nucleation of MnO_2 nanostructures. In summary, there are similarities in the configurations found in simulating metal oxides, namely, MnO_2, TiO_2, ZrO_2 and HfO_2 nanoclusters.

References

[1] Fernandes J B, Desai B D and Kamat Dalal V N 1984 *Electrochim. Acta* **29** 181
[2] Ghaemi M, Ghavami R K, Khosravi-Fard L and Kassaee M Z 2004 *J. Power Sources* **125** 256
[3] Wang D, Luo H, Kou R, Gill M P, Xiao S, Golub V O, Yang Z, Brinke C J and Lu Y 2004 *Angew. Chem. Int. Ed.* 436169
[4] Feng Z -P, Li G -R, Zhong J -H, Wang Z -L, Ou Y -N and Tong Y -X, *Electrochem. Commun.* 2009 **11** 706
[5] Karami H, Ramandi-Ghamoshi M, Moeini S and Salehi F 2010 *J. Clust. Sci.* **21** 21
[6] Jiao F and Bruce P G, *Adv. Mat.* 2007 **1**9 657
[7] Sayle T X T, Catlow C R A, Maphanga R R, Ngoepe P E and Sayle D C 2005 *J. Am. Chem. Soc.* **127** 12828
[8] Sayle T X T, Maphanga R R, Ngoepe P E and Sayle D C 2009 *J. Am. Chem. Soc.* **131** 6161
[9] Woodley S M and Catlow C R A 2008 *Nat. Mater.* **7** 937.
[10] Woodley S M, Applications of Evolutionary Computation in Chemistry, Berlin: Springer-Verlag Berlin, 2004
[11] Woodley S M, Battle P D, Gale J D and Catlow C R A 1999 *Phys. Chem. Chem. Phys.* **1** 2535
[12] Woodley S M, Battle P D, Gale J D and Catlow C R A, 2004 *Phys. Chem. Chem. Phys.* **6** 1815
[13] Woodley S M 2007 *Phys. Chem. Chem. Phys.* **9** 1070
[14] Woodley S M and Catlow C R A 2009 *Comput. Mater. Sci.* **45** 84
[15] Schön J C 2004 *Z. Anorg. Allg. Chem.* **630** 2354
[16] Roberts C and Johnston R L 2001 *Phys. Chem. Chem.* Phys. **3** 5024
[17] Al-Sunaidi A A, Sokol A A, Catlow C R A and Woodley S M 2008 *J. Phys. Chem. C* **112** 18860
[18] Woodley S M, Sokol A Aand Catlow C R A 2004 *Z. Anorg. Allg. Chem.* **630** 2343
[19] Hamad S, Woodley S M and Catlow C R A 2009 *Mol. Simul.* **35** 1015
[20] Flikkema E and Bromley S T 2004 *J. Phys. Chem. B* **108** 9638
[21] Woodley S M, Hamad S and Catlow C R A 2010 *Phys. Chem. Chem. Phys.* **12** 8454
[22] Walsh A and Woodley S M 2010 *Phys. Chem. Chem. Phys.***12** 8446
[23] Pinna N and Niederberger M 2008 *Angew. Chem. Int. Ed.* 47 5292
[24] Lai M and Riley D J 2008 *J. Colloid Interface Sci.* **323** 203
[25] Thomas J M and Midgley P A 2004 *Chem. Commun.* **11** 1253
[26] Möbus G and Inkson B J 2007 *Mater. Today* **10** 18
[27] Lai M, Kulak A N, Law D, Zhang Z B, Meldrum F C and Riley D J M. Lai 2007 *Chem. Commun.* **34** 3547
[28] Feng X D, Sayle D C, Wang Z L, Paras M S, Santora B, Sutorik A C, Sayle T X T, Yang Y, Ding Y, Wang X D and Her Y S 2006 *Science* **312** 1504
[29] Berry C C 2005 *J. Mater. Chem.* **15** 543
[30] Tarnuzzer R W, Colon J, Patil S and Seal S, *Nano Lett.* **5** 2573
[31] Maphanga R R, Parker S C and Ngoepe P E 2009 *Surf. Sci.* **603** 3184
[32] Ammundsen B, Islam M S, Jones D J and Rozière J 1999 *J. Power Sources* **81-82** 500
[33] Gale J D and Rohl A L 2003 *Mol. Simul.* **29** 291
[34] Havu V, Blum V, Havu P and Scheffler M 2009 *J. Comput. Phys.* **228** 8367
[35] Ngoepe P E, Maphanga R R and Sayle D C 2013 Computational Approaches to Energy Materials, Wiley & Sons, UK
[36] Francisco E, Martín Pendás A and Blanco M A 2005 *J. Chem. Phys.* **123** 234305
[37] Hamad S, Catlow C R A, Woodley S M, Lago S and Mejias J A 2005 *J. Phys. Chem. B* **109** 15741
[38] Hagfeldt A, Bergstroöm R, Siegbahn H O G and Lunell S 1993 *J. Phys. Chem.* **97** 12725
[39] Yu W and Freas R B 1990 *J. Am. Chem. Soc.* **112** 7126